BASIC PROPERTIES OF MUTUAL MAGNETIC HELICITY

P. DEMOULIN[1], E. PARIAT[1], M.A. BERGER[2]
[1] *Observatoire de Paris, LESIA, FRE 2461 (CNRS), F-92195 Meudon Principal Cedex, France* (pascal.demoulin@obspm.fr,etienne.pariat@obspm.fr)
[2] *Department of Mathematics, University College London* (m.berger@ucl.ac.uk)

Received ; accepted

Abstract. We derive the magnetic helicity for configurations formed by flux tubes contained fully or only partially in the spatial domain considered (called closed and open configurations, respectively). In both cases, magnetic helicity is computed as the sum of mutual helicity over all possible pairs of magnetic flux tubes weighted by their magnetic fluxes. We emphasize that these mutual helicities have properties which are **not** those of mutual inductances in classical circuit theory. For closed configurations, the mutual helicity of two closed flux tubes is their relative winding around each other (known as the Gauss linkage number). For open configurations, the magnetic helicity is derived directly from the geometry of the interlaced flux tubes so it can be computed without reference to a ground state (such as a potential field). We derive the explicit expression in the case of a planar and spherical boundary. The magnetic helicity has two parts. The first one is given only by the relative positions of the flux tubes on the boundary. It is the only part if all flux tubes are arch-shaped. The second part counts the integer number of turns each pair of flux tubes wind about each other. This provides a general method to compute the magnetic helicity with discrete or continuous distributions of magnetic field. The method sets closed and open configurations on an equal level within the same theoretical framework.

Keywords: magnetic fields, corona

1. Introduction

Magnetic helicity quantifies how the magnetic field is sheared and/or twisted compared to its lowest energy state (potential field). Observations of sheared, and even helical, magnetic structures in the photosphere, corona and solar wind have attracted considerable attention, with the consequent interest in magnetic helicity studies (see reviews in Brown, Canfield and Pevtsov, 1999, and, Berger, 2003). Stressed magnetic fields are often observed in association to flares, eruptive filaments, and coronal mass ejections (CMEs), but the precise role of magnetic helicity in such activity events still needs to be clarified.

Magnetic helicity plays a key role in magnetohydrodynamics (MHD) because it is almost preserved on a timescale less than the global diffusion timescale (Berger, 1984). Its conservation defines a constraint to


© 2005 *Kluwer Academic Publishers. Printed in the Netherlands.*

the magnetic field evolution; in particular a stressed magnetic field with finite total helicity cannot relax to a potential field. Thus magnetic helicity is at the heart of several MHD relaxation theories, for example of coronal heating (Heyvaerts and Priest, 1984) but also of flares (Kusano et al., 2004; Melrose, 2004). The permanent accumulation of helicity in the corona could be vital to the origin of CMEs (Rust, 1994; Low, 1997). In the convection zone, the accumulation of helicity in large scales limits the efficiency of the dynamo, thus the conservation of magnetic helicity is responsible of the dynamo saturation, the so-called α-effect quenching (Brandenburg, 2001).

Only relatively recently, it has been realized that magnetic helicity can be derived directly from observations. Presently the flux of magnetic helicity at the photospheric level is computed from the evolution observed in longitudinal magnetograms (Chae et al., 2004; Kusano et al., 2002; Nindos et al., 2003). The coronal helicity is estimated from magnetic extrapolation (Démoulin et al., 2002), while the helicity ejected in magnetic clouds (interplanetary counter part of CMEs) is derived through modelling the in-situ magnetic field measurements (Dasso et al., 2003). Thus, solar physicists have recently started quantitative studies relating the magnetic helicity observations from three domains: photosphere, corona and interplanetary medium. Statistical studies have been realized following the long-term CME activity of several active regions (Démoulin et al., 2002; Green et al., 2002; Nindos et al., 2003). In particular it was shown that differential rotation is not the main actor in the physics of CMEs. More recently a detailed study related a well observed small CME to an observed small magnetic cloud (Mandrini et al., 2005).

Despite the above recent advancements, only a fraction of the theoretical development has been applied to observations. This situation partly takes its origin in the fact that magnetic helicity is usually defined with the magnetic vector potential, a quantity which is far from any observed quantity. Moreover the computation of magnetic helicity could be lengthy and tricky. Several ways are usually possible but they are not equivalent in terms of complexity and application to presently available observations. A promising approach is to compute mutual helicity between flux tubes. The aim of this paper is to present such a procedure to compute coronal helicity. The main advantage is that computing mutual helicities can be done only using observable quantities.

We proceed progressively from the simplest cases, closed flux tubes (Section 2), to cases applicable to coronal configurations where magnetic flux cross the boundary of the computation domain (configurations called open, Section 3). For the close configurations we analyze

the formal parallel between mutual helicity and mutual inductance (as defined in circuit theory) and we emphasize the important differences (Section 2.4). The mutual helicity is directly related to the linkage number of the flux tubes. For open configurations, we cannot use directly the linkage number. We rather build the magnetic configuration by progressively bringing together elementary flux tubes. We use the injection of helicity with boundary motions (Section 3.2) to compute the helicity of both discrete and continuous distributions of flux tubes (Section 3.3). These results are derived in Cartesian geometry, and the equivalent derivation in spherical geometry is given in Appendix A. We then operate to remove the history of this building phase (paths of the flux tubes) in order to derive the helicity just from the final configuration. There are several caveats in this procedure (Section 3.4). The results are illustrated by computing the helicity of two magnetic flux tubes (Sections 3.5 & 3.6). It provides also the building block for deriving the helicity of both discrete and continuous distributions of flux tubes (Section 3.7). The symmetry properties of mutual helicity are analyzed in Section 4. Then we conclude on the properties of mutual helicity and on deriving coronal helicity (Section 5).

2. Closed configurations

Let us consider in this section closed configurations both for the current density $\mathbf{j}$ and the magnetic field $\mathbf{B}$, i.e. both are confined inside the volume $\mathcal{V}$ (which could be as large as needed). Both current lines and field lines are supposed to be closed on themselves, so we can define current channels and closed flux tubes. The main aim is to compare the properties of classical mutual inductance to the properties of mutual magnetic helicity: It also provides a base which will be used for open configurations (Section 3.6).

2.1. Magnetic energy

The magnetic energy of any field $\mathbf{B}$ contained inside $\mathcal{V}$ is:

$$E = \frac{1}{2\mu_0} \int_{\mathcal{V}} B^2 \, \mathrm{d}^3x = \frac{1}{2} \int_{\mathcal{V}} \mathbf{j} \cdot \mathbf{A} \, \mathrm{d}^3x \,, \tag{1}$$

where the vector potential $\mathbf{A}$ satisfies $\mathbf{B} = \nabla \times \mathbf{A}$. The second equality in Equation (1) suppose that $\int_{\mathcal{S}} \mathbf{A} \times \mathbf{B} \, \mathrm{d}^2x = 0$, where $\mathcal{S}$ is the boundary of $\mathcal{V}$. The vector potential $\mathbf{A}$ can be written as a function of $\mathbf{j}$; with the Coulomb gauge, $\nabla \cdot \mathbf{A} = 0$, we have:

$$\mathbf{A} = \mu_0 \int_{\mathcal{V}} \frac{\mathbf{j}(\mathbf{x}')}{|\mathbf{x} - \mathbf{x}'|} \, \mathrm{d}^3x' \,. \tag{2}$$

Then the magnetic energy can be written as a function of the currents alone:

$$E = \frac{\mu_0}{2} \int_{\mathcal{V}} \int_{\mathcal{V}} \frac{\mathbf{j}(\mathbf{x}) \cdot \mathbf{j}(\mathbf{x}')}{|\mathbf{x} - \mathbf{x}'|} \, \mathrm{d}^3x \, \mathrm{d}^3x' \,. \tag{3}$$

An approximation of this double integral can be realized by splitting the currents in N channels (with N as large as needed):

$$E \approx \frac{1}{2} \left(\sum_{i=1}^{N} L_i I_i^2 + \sum_{i=1}^{N} \sum_{j=1, j \neq i}^{N} M_{i,j} I_i I_j \right) , \tag{4}$$

where I_i & L_i are the current and the self-inductance of current channel i respectively, and $M_{i,j}$ is the mutual inductance between current channels i and j.

2.2. Magnetic helicity

The magnetic helicity of the field $\mathbf{B}$ fully contained within a volume $\mathcal{V}$ (i.e. at any point of $\mathcal{S}$ the normal component $B_n = \mathbf{B} \cdot \hat{\mathbf{n}}$ vanishes) is (Elsasser, 1956):

$$H^{\mathrm{close}} = \int_{\mathcal{V}} \mathbf{A} \cdot \mathbf{B} \, \mathrm{d}^3x \,. \tag{5}$$

The vector potential $\mathbf{A}$ can be written in function of $\mathbf{B}$ within the Coulomb gauge:

$$\mathbf{A}(\mathbf{x}) = \frac{1}{4\pi} \int \mathbf{B}(\mathbf{x}') \times \frac{(\mathbf{x} - \mathbf{x}')}{|\mathbf{x} - \mathbf{x}'|^3} \, \mathrm{d}^3x' \,. \tag{6}$$

Then the magnetic helicity can be written in function of $\mathbf{B}$ alone (Moffatt, 1969):

$$H^{\mathrm{close}} = \frac{1}{4\pi} \int_{\mathcal{V}} \int_{\mathcal{V}} \mathbf{B}(\mathbf{x}) \times \mathbf{B}(\mathbf{x}') \cdot \frac{(\mathbf{x} - \mathbf{x}')}{|\mathbf{x} - \mathbf{x}'|^3} \, \mathrm{d}^3x \, \mathrm{d}^3x' \,. \tag{7}$$

An approximation of this double integral can be realized by splitting the magnetic field in N flux tubes (Berger and Field, 1984):

$$H^{\mathrm{close}} \approx \sum_{i=1}^{N} T_i^{\mathrm{close}} \Phi_i^2 + \sum_{i=1}^{N} \sum_{j=1, j \neq i}^{N} \mathcal{L}_{i,j}^{\mathrm{close}} \Phi_i \Phi_j \,. \tag{8}$$

where Φ_i & T_i^{close} are the magnetic flux and the self helicity of flux tube i respectively (T_i^{close} includes both twist and writhe), and $\mathcal{L}_{i,j}^{\mathrm{close}}$ is the mutual helicity between flux tubes i and j.

2.3. Link between E and H with force-free fields

The two previous sections show that a formal parallel can be drawn between the computations of energy and helicity. This analogy is even stronger with force-free fields where:

$$\mathbf{j}(\mathbf{x}) = \frac{\alpha(\mathbf{x})}{\mu_0}\mathbf{B}(\mathbf{x})\,. \tag{9}$$

In this case H^{close} and E have similar expressions since Equation (5) has only an extra multiplicative factor $2\mu_0/\alpha(\mathbf{x})$ in the integrand compared to Equation (1).

Can we go further in this formal parallel ? More precisely, can we relate mutual helicities to mutual inductances ? Let consider a configuration formed by N discrete and thin current channels. Following Melrose (2004), this relation, if present, would be stronger in the case of a force-free field configuration since each current channel is also a flux tube. Let us further suppose that α is uniform in each channel ($\alpha = \alpha_i$). Then the current I_i of each current channel is related to the magnetic flux, Φ_i, along the corresponding flux tube by:

$$I_i = \alpha_i \Phi_i / \mu_0 \tag{10}$$

Then Equation (4) can be rewritten as:

$$E = \frac{1}{2\mu_0^2}\left(\sum_{i=1}^{N}\alpha_i^2 L_i \Phi_i^2 + \sum_{i=1}^{N}\sum_{j=1,j\neq i}^{N}\alpha_i\alpha_j M_{i,j}\Phi_i\Phi_j\right)\,. \tag{11}$$

One can also rewrite the right-hand side of Equation (1) using the force-free equation:

$$E = \frac{1}{2\mu_0}\int_{\mathcal{V}}\alpha\mathbf{B}\cdot\mathbf{A}\;\mathrm{d}^3x\,. \tag{12}$$

As for Equation (5), an approximation of this double integral can be realized by splitting the magnetic field in N flux tubes:

$$E = \frac{1}{2\mu_0}\left(\sum_{i=1}^{N}\alpha_i T_i^{\text{close}}\Phi_i^2 + \sum_{i=1}^{N}\sum_{j=1,j\neq i}^{N}\alpha_i\mathcal{L}_{i,j}^{\text{close}}\Phi_i\Phi_j\right)\,. \tag{13}$$

Next, let us suppose that the Φ_i are independent variables, and that $L_i, M_{i,j}, T_i, \mathcal{L}_{i,j}^{\text{close}}$ are not functions of the Φ_i. Then comparing Equation (11) and Equation (13) term by term in $\Phi_i\Phi_j$, and using the symmetries $M_{i,j} = M_{j,i}$ and $\mathcal{L}_{i,j}^{\text{close}} = \mathcal{L}_{j,i}^{\text{close}}$, we have:

$$T_i^{\text{close}} = \frac{\alpha_i}{\mu_0}L_i \quad ; \quad \mathcal{L}_{i,j}^{\text{close}} = \frac{2}{\mu_0}\frac{\alpha_i\alpha_j}{\alpha_i+\alpha_j}M_{i,j}\,, \tag{14}$$

The above derivation reaches the conclusion that, for a force-free field, there is a direct proportionality between self/mutual helicities and self/mutual inductances, while different properties were derived previously (Berger, 1999 and references therein). In fact the above derivation is not correct because Equations (11) and (13) do not describe magnetic configurations with the same N elements, as follows. Equation (11), derived from Equation (4), uses N current channels while Equation (13) uses N magnetic flux tubes with the same spatial extension. The problem lies in the fact that when discretizing in N current channels, each channel of current I_i, does not only produce the magnetic field Φ_i along itself, as present in Equation 10, but it also creates a magnetic field outside its own volume (there is no return current at the periphery to shield the magnetic field created by the direct current I_i, as supposed in Equation 10). This induced magnetic field, outside the current channel, is responsible for the mutual inductance of two current tubes which are not linked (in the sense of the Gauss linking number). In contrast, the magnetic flux tube, shearing the same volume than the current channel I_i, does not have any magnetic field in the outside volume. Thus the current-channel description is not equivalent to the magnetic flux-tube description. When comparing Equations (11) and (13), since we use different descriptions, i.e. different bases, it is not possible to equalize the mutual terms as written in Equation (14).

Let us use only the current-channel description; then the approximation of Equation (12) is changed because for each current channel we need to take into account the potential field created outside. Let us approximate this outside field by K flux tubes, then the total magnetic field of each current channel is described by $K+1$ flux tubes with fluxes Φ_{k_i} (with $\Phi_{k_{i=1}} = \Phi_i$ for current channel i), so Equation (13) is replaced by:

$$E = \frac{1}{2\mu_0} \left(\sum_{i=1}^{N} \alpha_i T_i^{\text{close}} \Phi_i^2 + \sum_{i=1}^{N} \sum_{k_i=2}^{K+1} \alpha_i \mathcal{L}_{i,k_i}^{\text{close}} \Phi_i \Phi_{k_i} + \sum_{i=1}^{N} \sum_{j=1, j\neq i}^{N} \sum_{k_j=1}^{K+1} \alpha_i \mathcal{L}_{i,k_j}^{\text{close}} \Phi_i \Phi_{k_j} \right) . \quad (15)$$

There is only one extra summation (on k_j) since the other summation simplifies to one term as $\alpha = 0$ outside the current channel i. In the above derivation we keep the same representation, current channels, but then we cannot relate the mutual inductance and the mutual helicity of a couple of current channels (i, j), since we cannot compare term by term Equations (11) and (15).

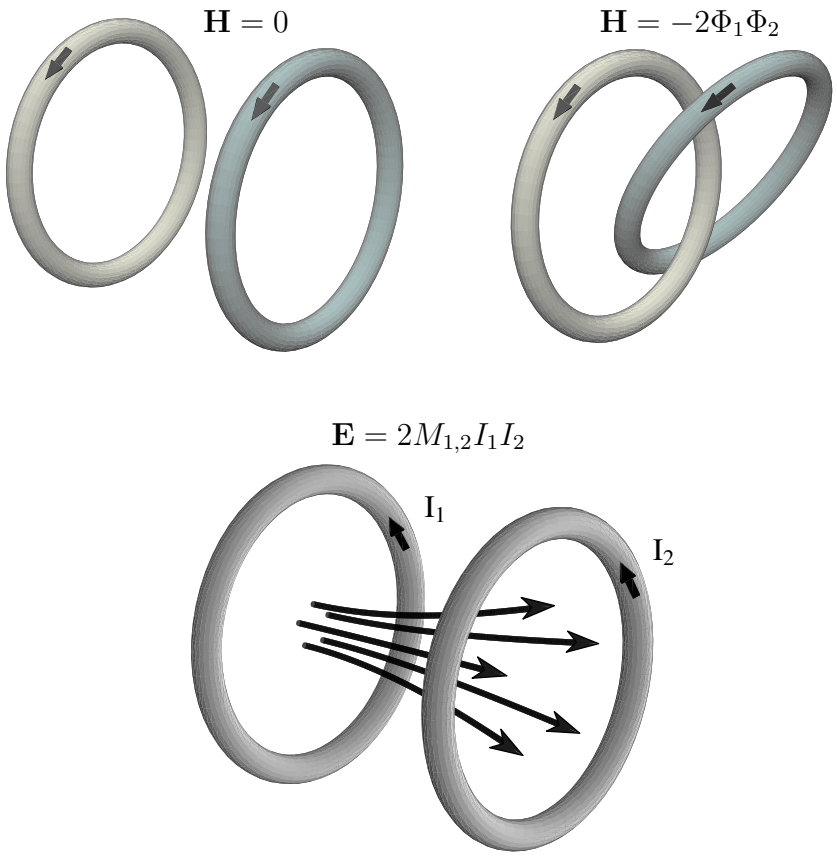


Figure 1. **Top**: two magnetic flux tubes. The magnetic helicity is twice the magnetic flux linkage $\mathcal{L}_{12}^{\rm close}$ ($= 0$ on the left, $= -1$ on the right) multiplied by the magnetic fluxes (Equations 8 and 17). **Bottom**: two current channels. The flux of the magnetic field created by one current channel, with unit current, through the current channel of the other current channel defines the mutual inductance M_{12}; thus the mutual inductance corresponds to the linkage of the magnetic flux created by one current channel with the second current channel (Equation 20).

We conclude that, even for a force-free field, there is no relationship between mutual inductances and mutual helicities. The above discussion points out the need for a clear derivation of mutual helicities (they cannot be approximated by Equation 13 of Melrose 2004). This will change the coefficients in the flare theory of Melrose, but we are not challenging here the global derivation of his flare model, but rather we proceed deriving the proper expressions for the mutual helicities.

2.4. Properties of mutual helicity and inductance

Let us rewrite Equation (7) by doing the integration along and across the elementary flux tubes. Each tube is defined by a close curve $\mathcal{C}$ along its axis and an elementary magnetic flux $\mathrm{d}\Phi$. The element of integration d^3x is replaced by $\mathrm{d}S\ \mathrm{d}l$, with $\mathbf{B}\ \mathrm{d}S = \hat{\mathbf{t}}\ \mathrm{d}\Phi$, and Equation (7) is rewritten as:

$$H^{\text{close}} = \int_{\Phi}\int_{\Phi} \mathcal{L}^{\text{close}}_{\mathcal{C},\mathcal{C}'}\ \mathrm{d}\Phi\ \mathrm{d}\Phi' \,, \tag{16}$$

with

$$\mathcal{L}^{\text{close}}_{\mathcal{C},\mathcal{C}'} = \frac{1}{4\pi}\oint_{\mathcal{C}}\oint_{\mathcal{C}'} \hat{\mathbf{t}}(\mathbf{x})\times\hat{\mathbf{t}}(\mathbf{x}')\cdot\frac{(\mathbf{x}-\mathbf{x}')}{|\mathbf{x}-\mathbf{x}'|^3}\ \mathrm{d}l\ \mathrm{d}l' \,. \tag{17}$$

$\mathcal{L}^{\text{close}}_{\mathcal{C},\mathcal{C}'}$ is known as the Gauss linking number of these two curves (Moffatt, 1969). It defines the number of times one curve turns around the other taking into account the orientations of the curves. $\mathcal{L}^{\text{close}}_{\mathcal{C},\mathcal{C}'}$ is a signed integer, invariant to deformations of the two curves which do not involve one curve passing through the other (but each curve is allowed to pass through itself). For two unlinked curves (which can be separated to infinitely large distance without crossing each other), one has $\mathcal{L}^{\text{close}}_{\mathcal{C},\mathcal{C}'} = 0$.

In the case of $\mathbf{B}$ localized in N flux tubes, Equation (16) simplifies to Equation (8) and Equation (17) provides an explicit way to compute the mutual helicity. The mutual inductance shares only one common property with the mutual helicity: both are symmetric, i.e. $M_{i,j} = M_{j,i}$ and $\mathcal{L}^{\text{close}}_{i,j} = \mathcal{L}^{\text{close}}_{j,i}$. Apart from that, their properties are very different. For example let us consider two unlinked flux tubes: they have $\mathcal{L}^{\text{close}}_{i,j} = 0$ independently of their distance or relative orientation, unlike the mutual inductance $M_{i,j}$ of two current channels which decreases progressively as the currents are more distant or as the current channels are less parallel (Figure 1).

The magnetic energy can also be written as a function of the Gauss linkage number, as follow. Just as $\mathbf{A}$ can be written as a function of $\mathbf{B}$ (Equation 6), one has:

$$\mathbf{B}(\mathbf{x}) = \frac{\mu_0}{4\pi}\int \mathbf{j}(\mathbf{x}')\times\frac{(\mathbf{x}-\mathbf{x}')}{|\mathbf{x}-\mathbf{x}'|^3}\ \mathrm{d}^3x' \,. \tag{18}$$

Included once in the magnetic energy definition, $E = \int_{\mathcal{V}} B^2/(2\mu_0)\ \mathrm{d}^3x$, we get:

$$E = \frac{1}{8\pi}\int_{\mathcal{V}}\int_{\mathcal{V}} \mathbf{B}(\mathbf{x})\times\mathbf{j}(\mathbf{x}')\cdot\frac{(\mathbf{x}-\mathbf{x}')}{|\mathbf{x}-\mathbf{x}'|^3}\ \mathrm{d}^3x\ \mathrm{d}^3x' \,. \tag{19}$$

Rewriting the integrations along magnetic flux tubes and currents located along the curves $\mathcal{C}$ and $\mathcal{C}'$ respectively, it transforms to:

$$E = \frac{1}{2} \int_{\Phi} \int_{I} \mathcal{L}^{\text{close}}_{\mathcal{C},\mathcal{C}'} \, \mathrm{d}\Phi \, \mathrm{d}I' \,. \tag{20}$$

It follows that the magnetic energy can be seen as the summation of the linkage between the magnetic flux and the current channels weighted by the elementary flux and currents. For example, with $\mu_0 = 1$, the mutual inductance $M_{i,j}$ of two current channels is the magnetic flux created by current channel i with unit current through the current channel j (or vice-versa). This property is pictured in Figure 1. As the distance between the two current channels increases, or as the current channels become less parallel, $M_{i,j}$ decreases as the magnetic flux though the current channel j does.

3. Magnetic helicity in open configurations

3.1. Relative magnetic helicity

The definition of the magnetic helicity with Equation (5) is limited to the cases when the magnetic field is fully contained inside the volume $\mathcal{V}$. In the case where $\mathcal{V}$ is part of the corona, we clearly have magnetic fluxes crossing $\mathcal{S}$, in particular for the part of $\mathcal{S}$ located at the photospheric level. Let us call B_n the normal field component at the boundary $\mathcal{S}$. Berger and Field (1984) have shown that for cases where $B_n \neq 0$ on $\mathcal{S}$ one can define a relative magnetic helicity, H, by subtracting the helicity of a reference potential field $\mathbf{B}_p$ which has the same B_n distribution on $\mathcal{S}$. A general expression for H is (Finn and Antonsen, 1985):

$$H = \int_{\mathcal{V}} (\mathbf{A} + \mathbf{A}_p) \cdot (\mathbf{B} - \mathbf{B}_p) \, \mathrm{d}^3x \,. \tag{21}$$

It is independent of the gauge selected for $\mathbf{A}$ and $\mathbf{A}_p$ since any change of gauge adds a term of the form $\nabla\Phi$ to $\mathbf{A} + \mathbf{A}_p$, and the extra integral vanishes because $B_n = B_{p,n}$ on $\mathcal{S}$.

3.2. Injection of helicity

With magnetic flux crossing the boundary $\mathcal{S}$ of the volume $\mathcal{V}$, we no longer have closed flux tubes so the approach of Section 2.4 to compute the magnetic helicity is not applicable. However we can keep track of the helicity flux crossing $\mathcal{S}$.

The flux of H through $\mathcal{S}$ can be written in general as (Berger and Field, 1984):

$$\frac{\mathrm{d}H}{\mathrm{d}t} = 2\int_{\mathcal{S}}[(\mathbf{A}_p\cdot\mathbf{B})v_n - (\mathbf{A}_p\cdot\mathbf{v})B_n]\ \mathrm{d}^2x\,, \tag{22}$$

where $\mathbf{v}$ is the plasma velocity and the subscript n indicates the component locally orthogonal to $\mathcal{S}$.

We assume below that the boundary $\mathcal{S}$ is planar (see Appendix A for a spherical boundary $\mathcal{S}$). In this geometry the field $\mathbf{A}_p$ is especially simple (Berger, 1984):

$$\mathbf{A}_p(\mathbf{x}) = \frac{\hat{\mathbf{n}}}{2\pi}\times\int_{\mathcal{S}} B_n(\mathbf{x}')\frac{\mathbf{x}-\mathbf{x}'}{|\mathbf{x}-\mathbf{x}'|^2}\ \mathrm{d}^2x'\,. \tag{23}$$

Let us define $\theta(\mathbf{x}-\mathbf{x}')$ as the angle between $\mathbf{x}-\mathbf{x}'$ and a fixed direction with trigonometric convention. The inclusion of Equation (23) in Equation (22) permits to write, after some computations (Berger, 1984):

$$\frac{\mathrm{d}H}{\mathrm{d}t} = 2\int_{\mathcal{S}}\int_{\mathcal{S}}\frac{\mathrm{d}\theta(\mathbf{x}-\mathbf{x}')}{\mathrm{d}t}\ B_n(\mathbf{x})B_n(\mathbf{x}')\ \mathrm{d}^2x\ \mathrm{d}^2x'\,. \tag{24}$$

This equation shows that the helicity injection rate can be understood as the summation of the rotation rate of all the pairs of elementary fluxes weighted with their magnetic flux.

The above double summations do not take into account how the magnetic field connects the positive ($B_n>0$) to the negative ($B_n<0$) flux regions of $\mathcal{S}$; however it is possible to rewrite the summations more explicitly in terms of the coronal connections. Let a be the label of a generic flux tube going from $\mathbf{x}_{a_+}$ to $\mathbf{x}_{a_-}$ with a flux $\mathrm{d}\Phi_a$. Similarly, the flux tube labeled c travels from $\mathbf{x}_{c_+}$ to $\mathbf{x}_{c_-}$ and has a flux $\mathrm{d}\Phi_c$. Thus Equation (24) can be rewritten as (Pariat et al., 2005):

$$\begin{aligned}\frac{\mathrm{d}H}{\mathrm{d}t} = \frac{1}{2\pi}\int_\Phi\int_\Phi\Bigg(&\frac{\mathrm{d}\theta(\mathbf{x}_{c_-}-\mathbf{x}_{a_+})}{\mathrm{d}t} + \frac{\mathrm{d}\theta(\mathbf{x}_{c_+}-\mathbf{x}_{a_-})}{\mathrm{d}t}\\ &-\frac{\mathrm{d}\theta(\mathbf{x}_{c_+}-\mathbf{x}_{a_+})}{\mathrm{d}t} - \frac{\mathrm{d}\theta(\mathbf{x}_{c_-}-\mathbf{x}_{a_-})}{\mathrm{d}t}\Bigg)\ \mathrm{d}\Phi_a\ \mathrm{d}\Phi_c\,.\end{aligned} \tag{25}$$

So, the input of helicity involve the summation, over all the pairs of flux tubes, of the relative rotation of their foot points.

3.3. Helicity computed with boundary motions

We can calculate the magnetic helicity of a configuration by progressively building up the configuration (by bringing elementary flux tubes

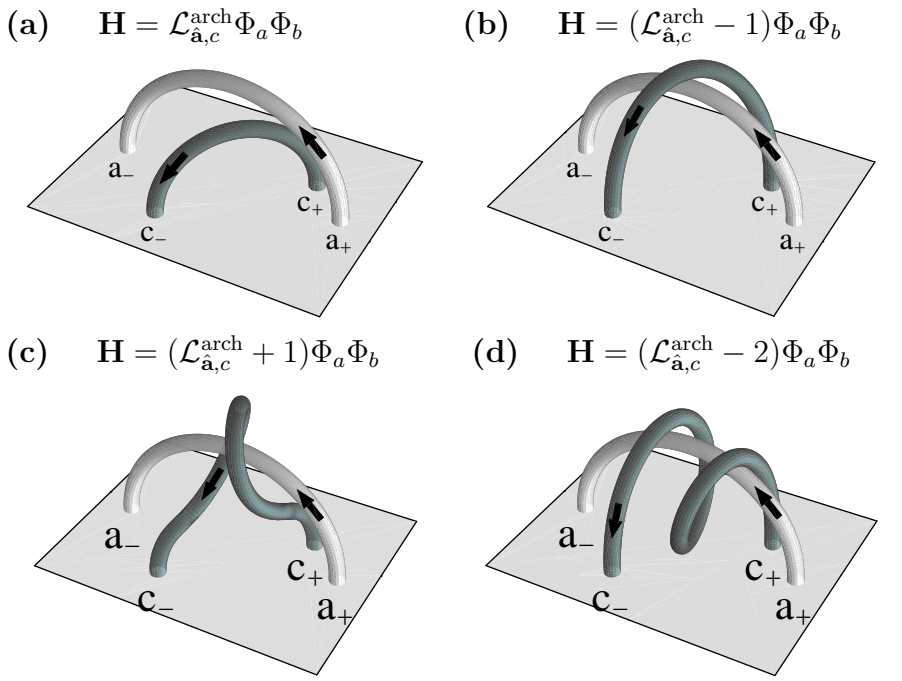


Figure 2. Examples of two magnetic flux tubes rooted at a_-,a_+ and c_-,c_+ respectively. **Top row:** Arch-like flux tubes. The left (right) panel shows the case where the flux tube "a" is above (below) the flux tube "c", respectively. The mutual helicity is given by $\mathcal{L}^{\rm arch}_{\hat{\mathbf{a}},c}$ (Equation 31) and $\mathcal{L}_{a,\hat{\mathbf{c}}} = \mathcal{L}^{\rm arch}_{\hat{\mathbf{a}},c} - 1$ (Equation 30) respectively. **Bottom row:** Linked flux tubes. These configurations can be created from the configurations on the top by rotating in the clockwise (trigonometric) direction the foot point c_+ by one turn around a_+ for the left (right) panels respectively (with some added ideal deformation to get the precise shape of flux tube "c". Equivalently c_- can be turned around a_-).

one after the other) and by summing up the helicity injection during the process. The helicity is formally equal to:

$$H = \frac{1}{2\pi}\int_\Phi\int_\Phi \mathcal{L}_{a,c}\,\mathrm{d}\Phi_a\,\mathrm{d}\Phi_c\,, \tag{26}$$

where $\mathcal{L}_{a,c}$ is the mutual helicity of the flux tubes "a" and "c" with:

$$\begin{aligned}\frac{\mathrm{d}\mathcal{L}_{a,c}}{\mathrm{d}t} \;=\; &\frac{\mathrm{d}\theta(\mathbf{x}_{c_-}-\mathbf{x}_{a_+})}{\mathrm{d}t} + \frac{\mathrm{d}\theta(\mathbf{x}_{c_+}-\mathbf{x}_{a_-})}{\mathrm{d}t} \\ &- \frac{\mathrm{d}\theta(\mathbf{x}_{c_+}-\mathbf{x}_{a_+})}{\mathrm{d}t} - \frac{\mathrm{d}\theta(\mathbf{x}_{c_-}-\mathbf{x}_{a_-})}{\mathrm{d}t}\,.\end{aligned} \tag{27}$$

The time integration of Equation (27) corresponds to the progressive building of the magnetic configuration. The electrostatic energy of a collection of charges is often calculated in a similar way, but unlike the

electrostatic case, flux tubes are not punctual elements, and we need to care not only about the two foot point motions but also about the 3D shape of the flux tubes these motions imply.

The computation of the magnetic helicity involves summing the helicity input over all possible pairs of elementary flux tubes (Equation 26). The difficulty lies only in our ability to compute the mutual helicity of a pair of flux tubes (so integrating Equation (27) in time).

Let us consider virtual motions which continuously deform the flux tubes. In particular we forbid the crossing of two flux tubes, just as in ideal MHD, so the allowed motions can simply be called ideal motions. Preserving the 3D topology of the flux tubes is important; when two flux tubes reconnect the mutual helicity is changed to self helicity (mainly twist in each flux tube, Wright and Berger, 1989). In principle it is possible to take this into account, but we avoid this since we want to compute the mutual helicity in the simplest possible way.

What are the motions needed to build a generic pair of flux tubes? In a first step we start from a generic pair of flux tubes "a" and "c" and look for the ideal motions needed to separate them to an infinite distance. In many cases we cannot separate them by simply translating rigidly one of the flux tubes: they are linked together. So first we need to unlink them by doing just enough relative rotation of the foot points a_- around c_- and/or a_+ around c_+. These rotations can be limited to an integer number of turns, bringing back the foot points to their initial positions but with a different 3D shape of the flux tubes (see examples in Figure 2). When flux tube "a" is no longer doing more than one turn around flux tube "c", the flux tubes can be "straightened" by ideal motions resulting in both having an arch-like shape (keeping the foot points at fixed positions). Then the flux tubes can be separated to an arbitrary large distance by simple translation motions. The computation of the mutual helicity proceeds with the reverse series of ideal motions: first translation then "unstraightening" and finally rotations (the last two can be reversed to get the final shape more easily).

We are now in position to compute the magnetic helicity. Let us consider two generic arch-like flux tubes "a" and "c" with "c" at infinitely large distance from "a". This configuration has zero helicity. Next move flux tube "c" into place with the three kinds of ideal motions defined above, keeping track of the helicity change (only the first and third motions change the helicity). From Equation (25) we need to integrate the variation of the position angle of foot points c_+, c_- as seen from a_+ and a_-, so let us use polar coordinates centered on a_+ (resp. a_-). The position of foot point c (either c_+ or c_-) with respect to a (either a_+ or a_-) is $\mathbf{x} = r(\cos\theta, \sin\theta)$, with $\theta = \theta_\infty$ when c is at infinity and $\theta = \theta_{ca}$ when c is in place. Here we need a continuous function θ, without any

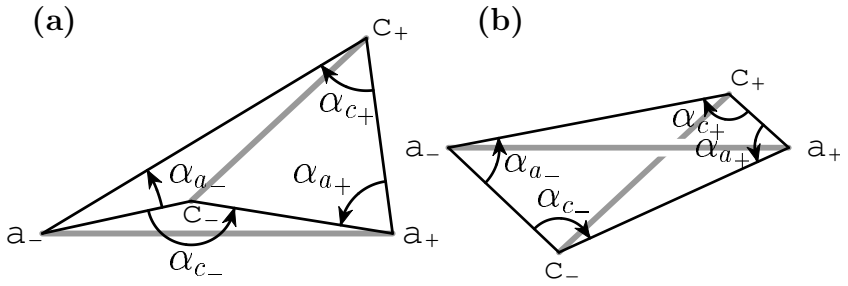


Figure 3. Definitions of the angles α for the mutual magnetic helicity of two flux tubes a & c (see Figure 2 for examples). The flux tubes are rooted on the boundary $\mathcal{S}$ at a_-, a_+ and c_-, c_+ respectively. There are two cases: **(a)** when the segments a_-a_+ and c_-c_+ do not intercept, and **(b)** when they do. The foot point positions can be described either by $(\alpha_{a_-}, \alpha_{a_+})$ or by $(\alpha_{c_-}, \alpha_{c_+})$. The angles are positive in the trigonometric direction: $\alpha_{a_-}, \alpha_{a_+} > 0$, $\alpha_{c_+} < 0$ in both panels, and $\alpha_{c_-} > 0$ (< 0) in the left (right) panel respectively. The right panel has the foot points localized as in Figure 2. Both panels are foot-point examples of those used in Figure 4.

branch cut, so it is a multi-valued function that we notate as θ^m. There are an infinite number of paths bringing "c" from infinity to its place, but for all the paths with ideal motions the change $\Delta\theta$ is $\theta_{ca} - \theta_\infty$. Thus, integrating Equation (27) in time, the mutual helicity for the two elementary flux tubes "a" and "c" is:

$$\mathcal{L}_{a,c} = \frac{1}{2\pi}(\theta^m_{c_+a_-} - \theta^m_{c_+a_+} + \theta^m_{c_-a_+} - \theta^m_{c_-a_-})\,. \tag{28}$$

The multi-valued function θ^m keeps track of how much foot points $c_\pm$ are rotating around foot points $a_\pm$ (and reciprocally), taking in account both translational and rotational motions.

3.4. Helicity computed with interior angles

In this section we apply the result of Equation (28) to translational motions (bringing the arch-like flux tube "c" in place from infinity). The aim is to simplify the practical use of Equation (28).

$\mathcal{L}_{a,c}$ is only an explicit function of the angles θ^m in the final configuration. Moreover, with **only** translational motions the angles θ^m change by less than one turn during the full transport. Hence it is tempting to compute the magnetic helicity just from the geometrical properties of the final configuration, i.e. from the single-value angles θ with a fixed reference direction. However, by forgetting the construction path, we lose the continuity of the functions θ^m: the function θ has a branch cut. The difficulty here is to define the location of the cut so that it does not affect Equation (28). In particular any difference of angles from each side of the branch cut will add a spurious value ± 1 to $\mathcal{L}_{a,c}$. In fact, it

is tricky to realize this generically for the four θ angles. For this reason we are not using Equation (28) with single-valued θ functions.

We can simplify the use of Equation (28) by defining the two interior angles (Berger, 1986):

$$\begin{aligned} \alpha_{c_+} &= \theta^m_{c_+a_+} - \theta^m_{c_+a_-} \\ \alpha_{c_-} &= \theta^m_{c_-a_-} - \theta^m_{c_-a_+}\,, \end{aligned} \tag{29}$$

with $\alpha_{c\pm}$ defined in the interval $[-\pi, \pi]$ so that $\alpha_{c\pm}$ is a single-valued function. They are both defined following two simple rules: one, the index of α (c_+ or c_-) indicates the vertex of the angle; two, the angle is oriented from the foot point of flux tube "a" with the same polarity sign (B_n sign) at the angle vertex towards the other foot point of "a" (with the trigonometric sign convention). Examples are shown in Figure 3. During the transport of flux tube "c", $\alpha_{c\pm}$ simply defines the angular extension of the segment a_-a_+ as seen from $c\pm$. If we restrict to the cases where the path of c_+ and c_- do not cross the segment a_-a_+ the function $\alpha_{c\pm}$ is a continuous function of the positions of c_+ and c_- and it is in the interval $[-\pi, \pi]$. With the definition of Equation (29) we define a new function:

$$\mathcal{L}^{\rm arch}_{a,\hat{\mathbf{c}}} = \frac{1}{2\pi}(\alpha_{c_+} + \alpha_{c_-})\,, \tag{30}$$

where the index $\hat{\mathbf{c}}$ indicates that the angles α are centered on the foot points of flux tube "c".

We could also have used the angles α centered on the foot points of flux tube "a". They define the angular extension of the segment c_-c_+ as seen from $a\pm$. With these angles we would then define the function:

$$\mathcal{L}^{\rm arch}_{\hat{\mathbf{a}},c} = \frac{1}{2\pi}(\alpha_{a_+} + \alpha_{a_-})\,. \tag{31}$$

Do we have the same mutual helicity with $\mathcal{L}^{\rm arch}_{\hat{\mathbf{a}},c}$ and $\mathcal{L}^{\rm arch}_{a,\hat{\mathbf{c}}}$? In fact there is an intrinsic asymmetry using the angles $\alpha_{a\pm}$ and $\alpha_{c\pm}$: $\alpha_{a\pm}$ is discontinuous by $\pm 2\pi$ when a_+ or a_- crosses the segment c_-c_+ while $\alpha_{c\pm}$ is also discontinuous by $\pm 2\pi$ but when c_+ or c_- crosses the segment a_+a_-. One example can be derived from Figure 3a: as c_- approaches the segment a_-a_+, α_{c_-} tends to π; but at the moment when c_- crosses a_-a_+, α_{c_-} jumps to $-\pi$. The above discontinuities imply a difference of 1 between $\mathcal{L}^{\rm arch}_{\hat{\mathbf{a}},c}$ and $\mathcal{L}^{\rm arch}_{a,\hat{\mathbf{c}}}$ in the region where the segments a_+a_- and c_-c_+ intercept each other, while $\mathcal{L}^{\rm arch}_{\hat{\mathbf{a}},c} = \mathcal{L}^{\rm arch}_{a,\hat{\mathbf{c}}}$ at other locations (Figure 4).

The above difference in the mutual helicities, $\mathcal{L}^{\rm arch}_{\hat{\mathbf{a}},c}$ and $\mathcal{L}^{\rm arch}_{a,\hat{\mathbf{c}}}$, is linked to an implicit difference in the magnetic configuration, as follows. Let us define the height as the distance to the boundary $\mathcal{S}$. Flux

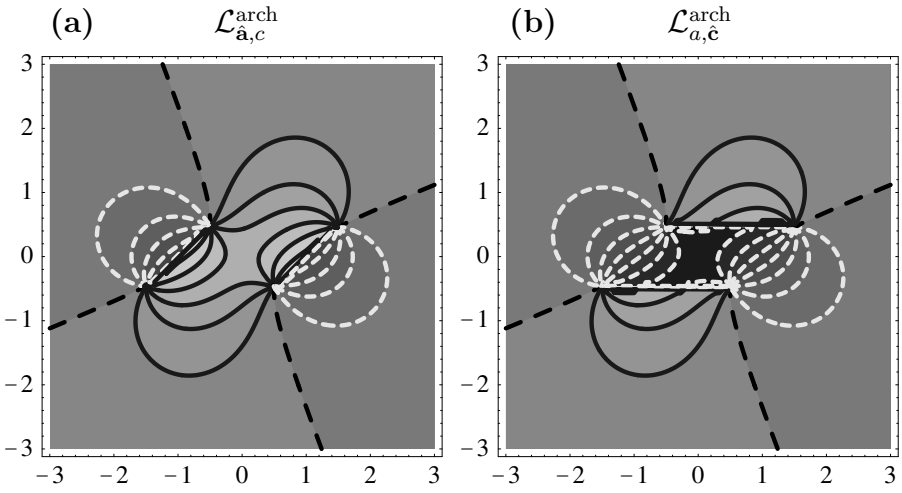


Figure 4. 2D plots of $\mathcal{L}^{\rm arch}_{\hat{\mathbf{a}},c}(x,y)$ and $\mathcal{L}^{\rm arch}_{a,\hat{\mathbf{c}}}(x,y)$ with (x,y) the coordinates of the middle of the segment c_-c_+. The foot points of flux tube "a" are fixed at a_- (-1,0) and a_+ (1,0), while the foot points of flux tube "c" are defined by $c_\pm$: $(x \pm \rho_c \cos\varphi_c, y \pm \rho_c \sin\varphi_c)$ with $\rho_c = 0.7$ and $\varphi_c = 0.75$ (the same values as in Figures 2 and 3). The positive (negative) values have black continuous (white dashed) isocontours respectively, while the zero value is black with long dashes. The isocontour values are separated by 0.1. The functions $\mathcal{L}^{\rm arch}_{\hat{\mathbf{a}},c}$ and $\mathcal{L}^{\rm arch}_{a,\hat{\mathbf{c}}}$ coincide except in the region where a_-a_+ and c_-c_+ intercept (central lozenge); there they differ by unity.

tube "c" is called "above" flux tube "a" when the closed curve defined by the elementary flux tube "c" and the segment c_-c_+ encircles flux tube "a". (In the case when flux tube "c" is in the plane defined by c_-c_+ and the normal $\hat{\mathbf{n}}$ to the boundary $\mathcal{S}$, flux tube "c" is strictly passing above flux tube "a"; this case can be generalized to any shape through an ideal deformation which keeps the foot points c_- and c_+ fixed since it does not change the mutual helicity). Let us analyze the mutual helicity evolution of $\mathcal{L}^{\rm arch}_{\hat{\mathbf{a}},c}$ when we set the arch-like flux tube "c" in place with ideal motions involving only translation. Flux tube "c" cannot be above flux tube "a" with a continuous evolution of the angles $\alpha_{a\pm}$ (as soon as the segment c_-c_+ cross a_- or a_+ there is a discontinuity of $\pm 2\pi$). Indeed when the segments a_+a_- and c_-c_+ intercept, the function $\mathcal{L}^{\rm arch}_{\hat{\mathbf{a}},c}$ implicitly selects the configuration where flux tube "a" is above flux tube "c", while it is the reverse for the function $\mathcal{L}^{\rm arch}_{a,\hat{\mathbf{c}}}$. An example of each case is shown in top panels of Figure 2, on the left for $\mathcal{L}^{\rm arch}_{\hat{\mathbf{a}},c}$ and on the right for $\mathcal{L}^{\rm arch}_{a,\hat{\mathbf{c}}}$.

We are now in position to compute the mutual helicity for a given pair of flux tubes with arch-like shapes. We simply need to determine

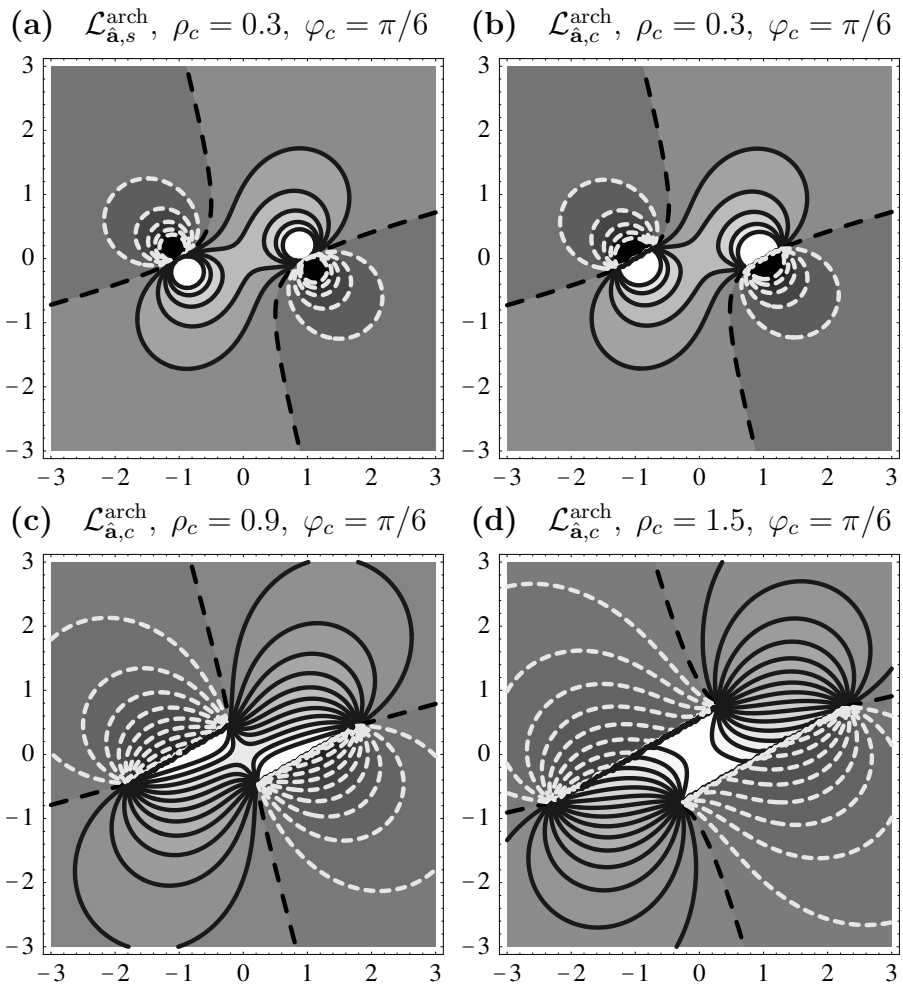


Figure 5. The mutual helicity $\mathcal{L}^{\rm arch}_{\hat{\mathbf{a}},c}$ for two arch-like flux tubes. The foot points $a\pm$ of flux tube "a" are fixed $(\pm 1, 0)$, while the foot point of flux tube "c" are defined by $c\pm = (x \pm \rho_c \cos\varphi_c, y \pm \rho_c \sin\varphi_c)$. The middle of the segment $c_- c_+$ is located at the position (x, y) of these 2D plots. ρ_c changes with the panel while φ_c has a fixed value. The top right panel is computed in the limit of very small flux tube "c" given by Equation (33). The isocontour values are equidistant by 0.05 and the drawing convention is the same as in Figure 4.

which one is above the other one (making the a/c symmetry explicit):

$$\begin{aligned} \mathcal{L}^{\rm arch}_{a,c} &= \mathcal{L}^{\rm arch}_{\hat{\mathbf{a}},c} && \text{if "a" above "c"} \\ &= \mathcal{L}^{\rm arch}_{a,\hat{\mathbf{c}}} && \text{if "c" above "a"} \\ &= \mathcal{L}^{\rm arch}_{\hat{\mathbf{a}},c} = \mathcal{L}^{\rm arch}_{a,\hat{\mathbf{c}}} && \text{otherwise}. \end{aligned} \tag{32}$$

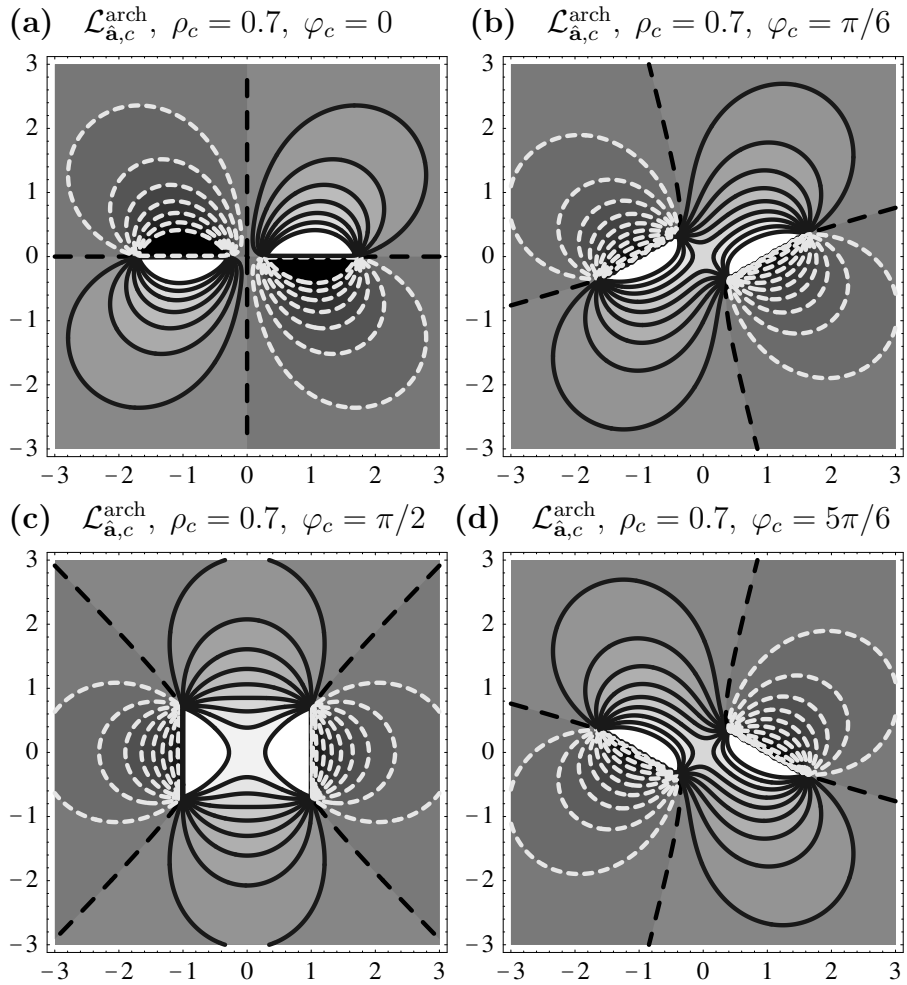


Figure 6. The mutual helicity $\mathcal{L}^{\rm arch}_{\hat{\mathbf{a}},c}(x,y)$ for two arch-like flux tubes. The drawing convention and the parameters are as in Figure 5 except that ρ_c is fixed, and φ_c changes with the panel.

3.5. Helicity of two arch-like flux tubes

In this part we analyze the behavior of the mutual helicity $\mathcal{L}^{\rm arch}_{\hat{\mathbf{a}},c}$ as a function of the relative position of two arch-like flux tubes "a" and "c". Without loss of generality we can select the system of coordinates on $\mathcal{S}$ such that the foot points of flux tube "a" are at $a\pm = (\pm 1, 0)$. The centre of the foot points of flux tube "c" is located at $(x,y) = (r\cos\varphi, r\sin\varphi)$. The segment c_-c_+ is angled by φ_c with respect to the x-axis, and it has a size $2\rho_c$.

When the flux tube "c" is small, $\rho_c \ll 1$, or far from "a", $\rho_c \ll r$, we can get a simple approximation of $\mathcal{L}^{\rm arch}_{\hat{\mathbf{a}},c}$ called $\mathcal{L}^{\rm arch}_{\hat{\mathbf{a}},s}$:

$$\mathcal{L}^{\rm arch}_{\hat{\mathbf{a}},s} = \frac{2\rho_c}{\pi} \frac{r^2 \sin(2\varphi - \varphi_c) + \sin\varphi_c}{(r^2-1)^2 + 4r^2\sin^2(\varphi)} \,. \tag{33}$$

In this limit the mutual helicity is proportional to the size ratio ρ_c of the flux tubes "c" and "a". Since "c" is supposed small compare to "a", $\mathcal{L}^{\rm arch}_{\hat{\mathbf{a}},s}$ implicitly assumes that "a" is above "c" when a_-a_+ and c_-c_+ intercept (central part of Figure 5a). However $\mathcal{L}^{\rm arch}_{\hat{\mathbf{a}},s}$ cannot be used around the branch cuts of $\mathcal{L}^{\rm arch}_{\hat{\mathbf{a}},c}$ (which have an extension proportional to ρ_c, so are small in the above context, even for $\rho_c = 0.3$ as shown by comparing Figures 5a and 5b).

The expression of $\mathcal{L}^{\rm arch}_{\hat{\mathbf{a}},s}$ simplifies at large distance, $r \gg 1$ and $2\varphi \neq \varphi_c$:

$$\mathcal{L}^{\rm arch}_{\hat{\mathbf{a}},s} \approx \frac{2\rho_c}{\pi r^2} \sin(2\varphi - \varphi_c) \,, \tag{34}$$

showing that the mutual helicity decreases relatively fast, as r^{-2} (the decrease is even faster, as r^{-4}, when $2\varphi = \varphi_c$). It captures also the main large scale properties of $\mathcal{L}^{\rm arch}_{a,c}$, which is formed by four lobes ($\sin(2\varphi)$ function) and which is rotated by $\varphi_c/2$ in the trigonometric direction (Figure 6).

In the opposite limit, $r \ll 1$:

$$\mathcal{L}^{\rm arch}_{\hat{\mathbf{a}},s} \approx \frac{2\rho_c}{\pi} \sin(\varphi_c) \,, \tag{35}$$

so, when flux tube "c" is located close to the centre of flux tube "a", the mutual helicity is defined simply by the relative orientation and size of the flux tubes.

When the flux tube "c" is not small, we get a simple expression when $r = 0$, i.e. when "c" is located precisely in the centre of "a": $\mathcal{L}^{\rm arch}_{a,c} = (1/\pi)\tan^{-1}[(2\rho_c \sin\varphi_c)/(1-\rho_c^2)]$ with $\tan^{-1}$ defined in the interval $[0,\pi]$. This expression reduces to Equation (35) when the $\tan^{-1}$ function can be approximate by its argument. This behavior is present in the central region of flux tube "a" (Figure 6). The largest mutual helicity is found when the two flux tubes are orthogonal (and not parallel as for mutual inductances, Section 2.4).

The two branch cuts of $\mathcal{L}^{\rm arch}_{\hat{\mathbf{a}},c}$, described in Section 3.4, are generically present. They are located where the segment c_-c_+ intercepts either a_+ or a_-, so they extend in size as ρ_c (Figure 5), and their orientation rotates with φ_c (Figure 6).

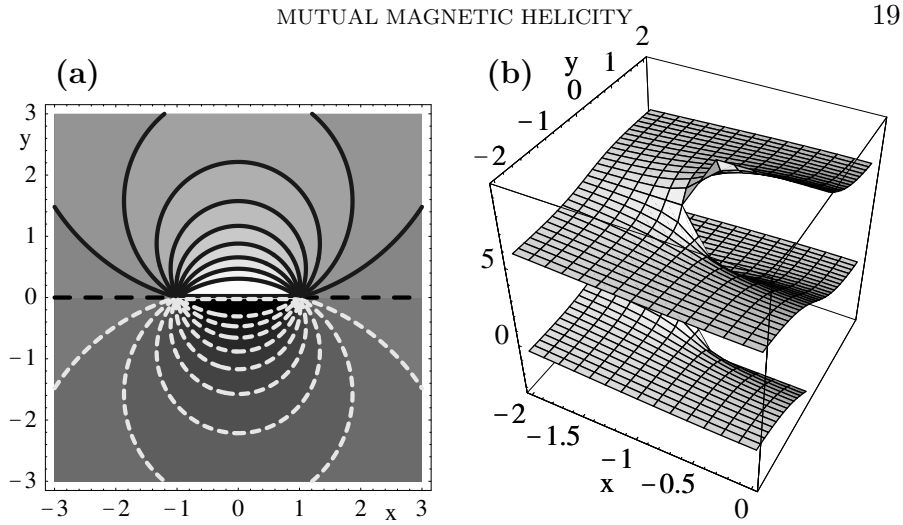


Figure 7. **(a)**: Isocontours of the single-value function α_{c_+} (same drawing convention as in Figures 4–6 with isocontour values separated by 0.1). **(b)**: 3D view of two layers of the multi-valued function $\alpha^m_{c_+}$. Only the negative x extension is drawn in order to better see the multi layers.

3.6. Helicity of two linked flux tubes

When two flux tubes are linked their mutual helicity does not only depend on their relative foot point positions but also on how much they turn around each other. Let us start with the example of Figure 2a and transform this configuration with an ideal motion where c_+ is rotating around a_+. After a rotation of one turn in the clockwise direction, the configuration is transformed to the one shown in Figure 2c (up to an ideal deformation keeping the foot points fixed). The mutual helicity has increased by unity (Equation 28). One can also transform the configuration of Figure 2a to those of Figure 2b with an ideal motion where c_+ is rotating around a_+ in the trigonometric direction. Another turn transforms Figure 2b to Figure 2d. Indeed, for the same foot point positions of flux tubes "a" and "c" the mutual helicity is $\mathcal{L}^{\rm arch}_{\hat{\mathbf{a}},c}+N$ where N is a signed integer representing the number of turns the flux tubes make around each other.

The case of linked flux tubes can be taken into account by generalizing the definition of α angles (Equation 29) to multi-valued functions α^m. Two layers of $\alpha^m_{c_+}$ are shown in Figure 7b: as c_+ turns around a_+ (or a_-) $\alpha^m_{c_+}$ progressively changes layer via the up/down connections present in the region around a_-a_+. An isocontour representation, as in Figures 4–6, of one layer is shown for comparison in Figure 7a. It has a branch cut on the segment a_-a_+. With both the positions of c_- and c_+ variable, $\mathcal{L}^{\rm arch}_{\hat{\mathbf{a}},c}$ and $\mathcal{L}^{\rm arch}_{a,\hat{\mathbf{c}}}$ have two cuts and their generalization with

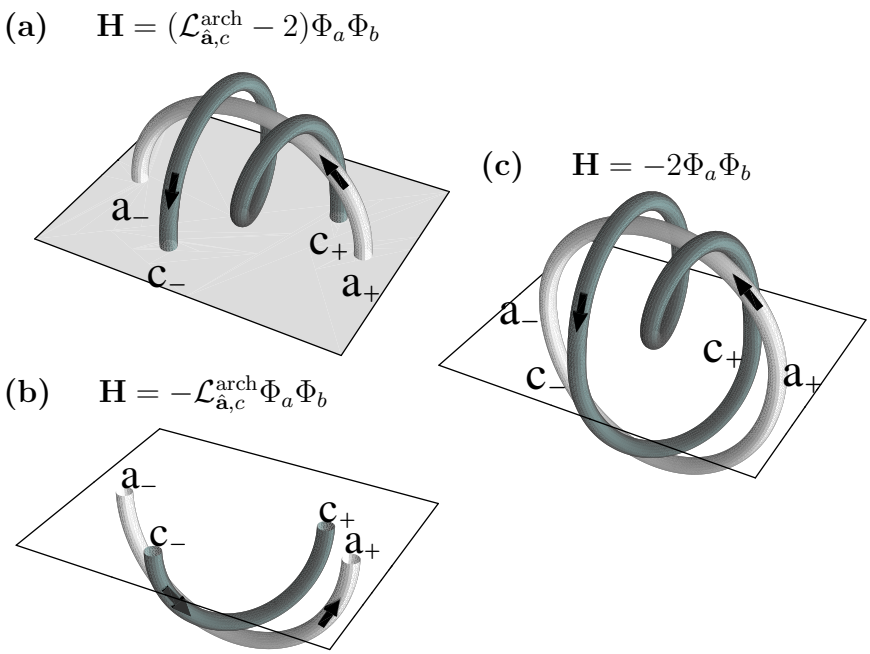


Figure 8. Computation of the magnetic helicity of the open configuration **(a)** is realized by closing it with the configuration **(b)** (the mirror image, through the boundary $\mathcal{S}$, of an arch-like configuration having the same foot-point locations as **(a)**). The sum of **(a)** and **(b)** gives the closed configuration **(c)**. The mutual helicity of **(b)** is computed with Equation (32) and those of the **(c)** is the Gauss linkage number (Equation 17). The mutual helicity of **(a)** is the difference between those of **(c)** and **(b)**.

α^m functions have the above multi-layer structure. These properties of the mutual helicity are even farther from the classical inductance properties than those described in Section 2.4 for closed flux tubes.

The difference between $\mathcal{L}^{\rm arch}_{\hat{\mathbf{a}},c}$ and $\mathcal{L}^{\rm arch}_{a,\hat{\mathbf{c}}}$ can also be understood with the multi-layer functions. When a_-a_+ and c_-c_+ do not intercept, $\mathcal{L}^{\rm arch}_{\hat{\mathbf{a}},c}$ and $\mathcal{L}^{\rm arch}_{a,\hat{\mathbf{c}}}$ coincide: they are in the same layer, that we will call the basic layer. However when a_-a_+ and c_-c_+ intercept we need a rotation with ideal motions of c_+ around a_+ (or c_- around a_-) by one turn to transform the configuration associated to $\mathcal{L}^{\rm arch}_{\hat{\mathbf{a}},c}$ (Figure 2a) to the one associated to $\mathcal{L}^{\rm arch}_{a,\hat{\mathbf{c}}}$ (Figure 2b). We find $\mathcal{L}^{\rm arch}_{a,\hat{\mathbf{c}}} = \mathcal{L}^{\rm arch}_{\hat{\mathbf{a}},c} - 1$. In that case $\mathcal{L}^{\rm arch}_{\hat{\mathbf{a}},c}$ and $\mathcal{L}^{\rm arch}_{a,\hat{\mathbf{c}}}$ are in the two connections attached to the basic layer and going to the neighbor layers: one is on the ascending connection and the other is on the descending connection.

The above multi-valued functions permit us to visualize the properties of the mutual helicity but they are not so efficient in practical

computations. It is more efficient to use the Gauss linkage number, as follows. For a generic configuration, $\mathcal{G}$, formed by two flux tubes "a" and "c" we first defined an arch-like configuration having the same foot-point locations. We then take its mirror image through the boundary $\mathcal{S}$ taking into account that the magnetic field is a pseudo vector, *i.e.* $B_x(-z) = -B_x(z)$, $B_y(-z) = -B_y(z)$, and $B_z(-z) = B_z(z)$ with (B_x, B_y, B_z) the three components of $\mathbf{B}$ in an orthogonal basis, where z is the coordinate orthogonal to the planar boundary located at $z = 0$. The mutual helicities of these configurations are $\mathcal{L}_{a,c}$ for the original configuration $\mathcal{G}$, $\mathcal{L}_{a,c}^{\rm arch}$ for the arch-like configuration, and $-\mathcal{L}_{a,c}^{\rm arch}$ for the mirror image of the arch-like configuration. Adding this arch-like mirror image to $\mathcal{G}$ permits us to close the initial configuration and thus to use the Gauss linkage number $\mathcal{L}_{a,c}^{\rm close}$ (Equation 17). So, the mutual helicity of the two initial flux tubes (configuration $\mathcal{G}$) is given by:

$$\mathcal{L}_{a,c} = \mathcal{L}_{a,c}^{\rm close} + \mathcal{L}_{a,c}^{\rm arch}\,, \tag{36}$$

with $\mathcal{L}_{a,c}^{\rm close}$ given by Equation (17) and $\mathcal{L}_{a,c}^{\rm arch}$ by Equation (32).

This general result is illustrated in Figure 8. Let compute the mutual helicity of the linked flux tubes shown in Figure 8a (configuration $\mathcal{G}$ above). Let first select the configuration of Figure 2a as the arch-like configuration with the same foot points. Its mirror image, Figure 8b, has a mutual helicity $-\mathcal{L}_{\hat{\mathbf{a}},c}^{\rm arch}$. Adding these two configurations gives two flux tubes linked by 2 turns (Figure 8c). Equation (36) gives directly the mutual helicity of $2 - \mathcal{L}_{\hat{\mathbf{a}},c}^{\rm arch}$ for the configuration of Figure 8a. We could equivalently have chosen to close the linked flux tubes with the image of the configuration shown in Figure 2b. The difference of 1 in the mutual helicity with the previously selected closing configuration is compensated by the same change in the Gauss linkage number of the closed configuration.

3.7. Helicity for a general magnetic configuration

We derive above a method for computing the mutual helicity of any pair of elementary flux tubes (Equation 36). Then by integrating Equation (26), we can compute the magnetic helicity of any open magnetic configuration above the boundary $\mathcal{S}$.

In the case of N discrete flux tubes with fluxes Φ_i, the integration of Equation (26) limited to each flux tube provides the self helicity $T_i\Phi_i^2$ (twist and writhe). The integration of Equation (26) limited to flux tube i and j gives $\mathcal{L}_{i,j}\Phi_i\Phi_j$. So, for N discrete flux tubes crossing the boundary $\mathcal{S}$ we get the same formal expression as for closed flux tubes

(Equation 8):

$$H = \sum_{i=1}^{N} T_i \Phi_i^2 + \sum_{i=1}^{N} \sum_{j=1, j\neq i}^{N} \mathcal{L}_{i,j} \Phi_i \Phi_j \,. \tag{37}$$

The main difference is that $\mathcal{L}_{i,j}$ is a continuous function of the foot point positions (Equation 36), contrasting with its integer value for closed flux tubes. If the extensions of flux-tube foot points are small compare with their separations, $\mathcal{L}_{i,j}$ is approximately the mutual helicity computed with the flux-tube axis. Finally, the self helicity T_i is not present in the continuous version of Equation (26) since the ratio of first summation to the second one in Equation (37) decreases as $1/N$, so becomes negligible for large N and null in the case of an integration.

4. Symmetry Properties

4.1. Mutual helicity with complex functions

The expression for mutual helicity, Equation (28), possesses several symmetries. We can derive these symmetries most easily by using complex variables. Assign complex numbers $z = x + iy$ to points on the photosphere (assumed to be a plane). Thus the positive foot point of arch a will be assigned the complex number a_+. Define a multi-valued complex logarithm $\log^m$ which satisfies

$$\frac{\mathrm{d}\log^m(z)}{\mathrm{d}z} = \frac{1}{z}, \tag{38}$$

but where the complex part is not restricted to the principal value (i.e. $|Im\ z|$ can be greater than π). Then, for example, we can write

$$\theta^m_{c_+a_-} = \mathcal{I}m\ \log^m(\mathsf{a}_- - \mathsf{c}_+). \tag{39}$$

The mutual helicity becomes

$$\mathcal{L}_{a,c} = \frac{1}{2\pi} \mathcal{I}m\ \log^m \left(\frac{(\mathsf{a}_+ - \mathsf{c}_-)(\mathsf{a}_- - \mathsf{c}_+)}{(\mathsf{a}_+ - \mathsf{c}_+)(\mathsf{a}_- - \mathsf{c}_-)} \right). \tag{40}$$

The object inside the complex logarithm is called a cross-ratio. These objects have many interesting properties (see, e.g. Conway, 1975). Given four complex numbers a, b, c, d, define

$$\mathcal{C}(\mathsf{a},\mathsf{b},\mathsf{c},\mathsf{d}) \;=\; \frac{(\mathsf{a}-\mathsf{c})(\mathsf{b}-\mathsf{d})}{(\mathsf{a}-\mathsf{d})(\mathsf{b}-\mathsf{c})}. \tag{41}$$

Then

$$\mathcal{L}_{a,c} = \frac{1}{2\pi}\mathcal{I}m\ \log^m \mathcal{C}(\mathsf{a}_+, \mathsf{a}_-, \mathsf{c}_-, \mathsf{c}_+). \tag{42}$$

Suppose we define the ordinary logarithm with a branch cut on the negative real axis. Then $\log^m \mathcal{C} = \log \mathcal{C} + n$ for some integer n counting the number of times the two tubes wrap around each other. The branch cut occurs when the sum of the angles equals π, for example when the each arch sits on the opposite corners of a square. If we ignore n, then we have a function just of the positions of the four foot points. This function obeys a set of symmetries called conformal symmetries.

4.2. Conformal symmetries

Given a complex number z, let the Möbius transformation $F(z)$ be defined by

$$F(z) = \frac{\alpha z + \beta}{\gamma z + \delta} \tag{43}$$

for some complex coefficients α, β, γ, and δ. Then a standard result in complex algebra shows that the cross ratio is invariant under this transformation. In other words,

$$\mathcal{C}(F(\mathsf{a}_+), F(\mathsf{a}_-), F(\mathsf{c}_-), F(\mathsf{c}_+)) = \mathcal{C}(\mathsf{a}_+, \mathsf{a}_-, \mathsf{c}_-, \mathsf{c}_+). \tag{44}$$

Thus the mutual helicity is preserved when all four foot point positions are acted upon by a Möbius transformation.

Conformal transformations (in the case of the complex plane, Möbius transformations) preserve angles. It is not surprising that they preserve mutual helicities, as these are built from angles. The simplest symmetries are

$$\begin{array}{ll} z \to \mathrm{e}^{i\theta} z, & \text{rotations;} \\ z \to z + \beta, & \text{translations;} \\ z \to r z & \text{dilations.} \end{array} \tag{45}$$

An additional, perhaps less obvious symmetry inverts points with respect to the unit circle:

$$z \to \frac{1}{z} \qquad \text{inversions.} \tag{46}$$

4.3. permutations

If we permute the four entries in the cross-ratio we obtain a new cross-ratio closely related to the original. For example, if

$$C_1 = \mathcal{C}(\mathsf{a}_+, \mathsf{a}_-, \mathsf{c}_-, \mathsf{c}_+) \tag{47}$$

then

$$C_2 \;=\; \mathcal{C}(\mathsf{c}_-, \mathsf{a}_+, \mathsf{a}_-, \mathsf{c}_+) = \frac{1}{1 - C_1} \tag{48}$$

$$C_3 \;=\; \mathcal{C}(\mathsf{a}_-, \mathsf{c}_-, \mathsf{a}_+, \mathsf{c}_+) = \frac{1}{1 - C_2} = \frac{C_1 - 1}{C_1}. \tag{49}$$

All other permutations give either C_1, C_2, C_3, or their inverses C_1^{-1}, C_2^{-1}, C_3^{-1}. For example, reversing a_+ and a_- gives

$$\mathcal{C}(\mathsf{a}_-, \mathsf{a}_+, \mathsf{c}_-, \mathsf{c}_+) = C_1^{-1}. \tag{50}$$

Upon taking the logarithm to obtain the mutual helicity, the negative exponent turns into a minus sign. This reflects the fact that reversing a_+ and a_- corresponds to reversing the direction of magnetic field for flux tube a.

5. Conclusion

The main aim of this work is to clarify the computation of magnetic helicity as the summation of mutual helicity over all pairs of flux tubes forming a given magnetic configuration. For that we revisit and extend the theory for both closed and open magnetic configurations. For the open case we consider only magnetic configurations bounded by a plane or a sphere representing, for example, a photospheric location. Extension to others boundary geometries are possible, simply technically more difficult.

We show that mutual helicity does **not** have the properties of mutual inductance even in the case of force-free fields ($\mathbf{j} = \alpha\mathbf{B}$), where magnetic field and current lines coincide, and even in magnetic configurations which are formed only of magnetic flux tubes closed on themselves (thus formally more comparable to current circuits than open magnetic configurations). The mutual helicity of two close flux tubes is defined by an integration along both flux tubes, known as the Gauss linkage number (Equation 17), which counts the number of times one flux tube turns around the other one. The mutual inductance of two closed current channels is instead the linkage of the magnetic flux created by one channel with the other channel.

When magnetic flux tubes cross the boundary $\mathcal{S}$ of the volume $\mathcal{V}$ where magnetic helicity is computed (the normal component $B_n \neq 0$ on $\mathcal{S}$), we cannot compute the Gauss linkage number. Moreover, we cannot simply limit the integration of Equation (17) to the parts inside $\mathcal{V}$: e.g. a simple example of pair of field lines limited to a finite $\mathcal{V}$, such

as those formed by a straight line and an helix, shows that the result is not correct. Instead we can compute the helicity by progressively forming the magnetic configuration: we successively bring elementary flux tubes of the configuration in place and count the helicity injected by tracking the foot point motions on $\mathcal{S}$. The mutual helicity of a pair of flux tubes has two parts: a first one which depends only on the position of the foot points on $\mathcal{S}$ and a second which counts how much the flux tubes wind around each other. The first part is a real number in the interval $]-1,1[$ and the second part is a signed integer.

We conclude that the magnetic helicity can be computed as the summation of the mutual helicity of all pairs of flux tubes multiplied by their fluxes. This approach is applicable both for configurations formed by discrete flux tubes (finite summation) and for configurations with continuous field (integration). However, the main difference is that we need to add the self helicities in the case of discrete flux tubes, while this contribution is included in the mutual helicities of the elementary flux tubes for a continuous configuration.

The method sets closed and open configurations on an equal level: in both cases we do not need to compute the reference potential field (although the results are always equivalent to Equation 21). Moreover, the helicity of closed configurations can be seen as a particular case of the helicity of open configurations: the contribution of the foot points simply disappears (the closed configuration can be formed by bringing the foot points of the associated open configuration together). On the other hand, we can close any open configuration by a field outside $\mathcal{V}$ which is formed only of arch-like flux tubes, and so we can associate to any open configuration a closed configuration. The helicity of the closing field can be computed only as a function of the foot point positions on $\mathcal{S}$. It provides the difference of helicities between the closed and open configurations.

The derived method does not rely on computing a vector potential field, but rather uses only observable quantities: the normal field component at the boundary and the flux tube linkages (connectivities and how each pair wind about each other). This will permit us to estimate more directly coronal magnetic helicities. The main concern here is the number of observable flux tubes. With a better spatial resolution and a larger temperature coverage, a larger number of loops will become observable. Solar-B mission, which will be launched in 2006, will provide a major step in this goal.

Appendix

A. Interior angles in spherical coordinates

We can employ the same techniques as Section 3.3 to derive expressions for the mutual helicity of two arches with foot points on a sphere. We will begin with flux tube "a" already in place, with foot points a_+ and a_- at arbitrary positions on the sphere. We cannot bring in elementary flux tube "c" from infinity, so instead we imagine it emerging through the surface, forming first a dipole then with c_+ and c_- moving away from each other until they reach their final positions. We then use Equation (22) to calculate the helicity input during this process. However, we need a new expression for $\mathbf{A}_p$ valid for a sphere of radius R.

Let $B_n(\theta, \phi)$ be the radial component of the field at the point of the surface of classical spherical coordinates (θ, ϕ).Then (Kimura and Okamoto, 1987) $\mathbf{A}_p = \hat{n} \times \nabla\psi$, where $\triangle\psi = -B_n$, with $\triangle$ being the surface Laplace operator (the Laplacian without the radial derivative term). The solution is

$$\psi(\theta, \phi) = -\frac{R^2}{4\pi} \oint B_n(\theta', \phi') \ln \frac{1 - \cos\xi}{2} \, d^2x', \tag{51}$$

where ξ is the spherical distance between (θ, ϕ) and (θ', ϕ'):

$$\cos\xi = \cos\theta' \cos\theta + \sin\theta' \sin\theta \cos(\phi - \phi'). \tag{52}$$

We can build up the field using a sum of magnetic point charges at the surface; these can be regarded as mathematical idealizations of intense photospheric flux elements. But we do not wish to have magnetic monopoles beneath the surface! A simple and effective method to prevent monopoles is to require that each surface magnetic charge be accompanied by a uniform return flux of opposite sign. Thus if the point charge has flux Φ_0, then the entire sphere outside the point is covered with a uniform field $B_n = -\Phi_0/(4\pi R^2)$. Note that if two equal and opposite point charges are placed on the sphere, their combined return fluxes cancel each other. This method makes the mathematical analysis easier, even if in the end the return fluxes all cancel out. (It also makes it easier to construct fields with n positive charges of net flux Φ, and m negative charges of net flux $-\Phi$, where $m \neq n$, although we will not need to do this here).

As a simple example, consider a magnetic point charge situated at the North pole. The field is

$$B_n = \frac{\Phi_0 \delta(\theta)}{2\pi R^2 \sin\theta} - \frac{\Phi_0}{4\pi R^2} \tag{53}$$

with $\delta(\theta)$ the Dirac delta function. This gives

$$\mathbf{A}_p = \frac{\Phi_0}{4\pi R}\frac{\sin\theta}{1-\cos\theta}\hat{\phi}. \tag{54}$$

Thus $\mathbf{A}_p$ points in the azimuthal direction, tracing out latitude lines. The integral of $\mathbf{A}_p$ around a latitude line equals the flux of the point charge, minus the return flux enclosed above the line.

Suppose the magnetic charge is instead placed at some arbitrary position $x' = (\theta', \phi')$. We will need a new spherical coordinate system (ξ, ψ) centred at (θ', ϕ'), with co-latitude $\xi = 0$ there, and ψ the azimuthal angle. Note that the choice for the location of $\psi = 0$ is arbitrary and can be chosen for convenience; however this will not affect our final results.

A point at position $x = (\theta, \phi)$ has coordinates (ξ, ψ) with ξ given by Equation (52), and ψ given by

$$\cot\psi_{x,x'} = \frac{\cos\theta'\cos(\phi-\phi') - \sin\theta'\cot\theta}{\sin(\phi-\phi')}. \tag{55}$$

Now suppose we place foot point a_+ at position $x' = (\theta', \phi')$, so at the origin of the spherical coordinates (ξ, ψ), and let flux tube "c" emerge and move to its final position. The net helicity input will be proportional to the interior spherical angle at a_+,

$$\alpha_{a_+} = \psi^m_{c_+,a_+} - \psi^m_{c_-,a_+}, \tag{56}$$

where the superscript m acknowledges that the angle might be multi-valued. (Thus the part of $\psi^m_{a_+,c_+}$ between $-\pi$ and π can be computed from Equation (55)).

The negative foot point a_- will also be present, so more angles $\psi^m_{c_+,a_-}$ and $\psi^m_{c_-,a_-}$ will have to be computed. Again these can be done using Equation (55) with (θ, ϕ) now corresponding to the position of a_-. The end result corresponding to Equations (28) and (31) is

$$\mathcal{L}_{a,c} = \frac{1}{2\pi}(\psi^m_{c_-,a_+} - \psi^m_{c_+,a_+} + \psi^m_{c_+,a_-} - \psi^m_{c_-,a_-}) \tag{57}$$

$$= \alpha_{a_+} + \alpha_{a_-}\,. \tag{58}$$

References

Berger, M. A.: 1984, *Geophys. Astrophys. Fluid Dyn.* **30**, 79.
Berger, M. A.: 1986, *Geophys. Astrophys. Fluid Dyn.* **34**, 265.

Berger, M. A.: 2003, in *Advances in Nonlinear Dynamos*, A. Ferriz-Mas and M. Núñez, eds., Gordon and Breach, p. 345
Berger, M. A. and Field, G.B.: 1984, *J. Fluid. Mech.* **147**, 133.
Berger, M.A.: 1999, in *Magnetic Helicity in Space and Laboratory Plasmas*, Geophys. Monograph 111, AGU, Washington DC, 1
Brandenburg, A.: 2001, *Astrophys. J.* **550**, 824.
Brown, M.R., Canfield, R.C., and Pevtsov, A.A. (eds.): 1999, Magnetic Helicity in Space and Laboratory Plasmas, Geophys. Mon. Ser. 111, AGU, Washington D.D.
Chae, J., Moon, Y., and Park, Y.: 2004, *Solar Phys.* **223**, 39.
Conway, J. B.: 1975, *Functions of One Complex Variable*, Springer-Verlag, New York.
Dasso, S., Mandrini, C.H., Démoulin, P., Farrugia, C.J.: 2003, *J. Geophys. Res.* **108**, 1362, SSH 3,1 doi:10.1029/2003JA009942.
Démoulin, P., Mandrini, C. H., van Driel-Gesztelyi, L., et al.: 2002, *Astron. Astrophys.* **382**, 650.
Elsasser, W. M.: 1956, *Rev. Mod. Phys.* **28**, 135.
Finn, J. H. and Antonsen, T. M.: 1985, *Comments Plasma Phys. Contr. Fusion* **9**, 111.
Green, L.M., López Fuentes, M.C., Mandrini, C.H., Démoulin, P., van Driel-Gesztelyi, L., and Culhane, J.L.: 2002, *Solar Phys.* **208**, 43.
Heyvaerts, J. and Priest, E.R.: 1984, *Astron. Astrophys.* **137**, 63.
Kimura, Y. and Okamoto, H.: 1987, J. Phys. Soc. Jpn. **56**, 2024.
Kusano, K., Maeshiro, T., Yokoyama, T., and Sakurai, T.: 2002, *Astrophys. J.* **577**, 501.
Kusano, K., Maeshiro, T., Yokoyama, T., and Sakurai, T.: 2004, *Astrophys. J.* **610**, 537.
Low, B.C.: 1997: in *Coronal mass ejections*, Geophysical Monograph 99, N. Crooker, J.A. Joselyn, J. Feynman (eds.), American Geophysical Press, p. 39
Mandrini, C.H., Pohjolainen, S., Dasso, S., Green, L.M, Démoulin, P., van Driel-Gesztelyi, L., Copperwheat, C., Foley, C.: 2005, *Astron. Astrophys.* **434**, 725.
Melrose, D.: 2004, *Solar Phys.* **221**, 121.
Moffatt, H. K.: 1969, J. Fluid Mech. **35**, 117.
Nindos, A., Zhang, J., and Zhang, H.: 2003, *Astrophys. J.* **594**, 1033.
Pariat, E., Démoulin, P., and Berger, M. A.: 2005, *Astron. Astrophys.* **439**, 1191.
Rust, D. M.: 1994, *Geophys. Res. Lett.* **21**, 241.
Wright, A. N. and Berger, M. A.: 1988, *J. Geophys. Res.* **94**, A2, 1295.